Reversibility of the structure and dewaterability of anaerobic digested sludge

Yiqi Sheng[1], Yili Wang[1],*, Wei Hu[1], Xu Qian[1], Huaili Zheng[2], Xiaoxiu Lun[1]

1. College of Environmental Science and Engineering, Beijing Key Lab for Source Control Technology of Water Pollution, Beijing Forestry University, Beijing 100083, China. E-mail: shengyiqi09@163.com
2. College of Urban Construction and Environmental Engineering, Chongqing University, Chongqing 400044, China

ABSTRACT

The reversibility of the structure and dewaterability of broken anaerobic digested sludge (ADS) is important to ensure the efficiency of sludge treatment or management processes. This study investigated the effect of continuous strong shear (CSS) and multipulse shear (MPS) on the zeta potential, size (median size, d_{50}), mass fractal dimension (D_F), and capillary suction time (CST) of ADS aggregates. Moreover, the self-regrowth (SR) of broken ADS aggregates during slow mixing was also analyzed. The results show that raw ADS with d_{50} of 56.5 μm was insensitive to CSS–SR or MPS–SR, though the size slightly decreased after the breakage phase. For conditioned ADS with d_{50} larger than 600 μm, the breakage in small-scale surface erosion changed to large-scale fragmentation as the CSS strength increased. In most cases, after CSS or MPS, the broken ADS had a relatively more compact structure than before and d_{50} is at least 200 μm. The CST of the broken fragments from optimally dosed ADS increased, whereas that corresponding to overdosed ADS decreased. MPS treatment resulted in larger and more compact broken ADS fragments with a lower CST value than CSS. During the subsequent slow mixing, the broken ADS aggregates did not recover their charge, size, and dewaterability to the initial values before breakage. In addition, less than 15% self-regrowth in terms of percentage of the regrowth factor was observed in broken ADS after CSS at average velocity gradient no less than 1905.6 sec^{-1}.

© 2015 The Research Center for Eco-Environmental Sciences, Chinese Academy of Sciences. Published by Elsevier B.V.

Introduction

Sewage sludge consists of microbial organisms and colonies, extracellular polymeric substances (EPS) and inorganic matter. The microorganisms are embedded in the gel-like matrix of EPS, which is further linked by EPS to form the flocs or aggregates of sewage sludge (Dursun, 2007). Coagulation or flocculation conditioning is an important process for sewage sludge dewatering, and the applied shear during and after conditioning is crucial for effective conditioning. In general, additional shear is created in

pipes, pumps, in-line flow meters, and even dewatering devices during sewage sludge treatment and management. According to the previous studies (Novak et al., 1988; Novak and Bandak, 1989; Novak, 1990; Abu-Orf and Dentel, 1997; Örmeci and Ahmad, 2009), the additional shear breaks flocs and exposes the negatively charged fresh surfaces, which in turn increase the polymer demand of sewage sludge conditioning. Moreover, Örmeci and Ahmad (2009) indicated that additional shearing after conditioning had a significant effect on the optimum polymer dose, even doubling the polymer dose required for conditioning of the broken sludge flocs after an in-line flow meter (Werle et al., 1984). Therefore, Örmeci and Ahmad (2009) determined the variations

of the measured torque values for conditioned anaerobic digested sludge (ADS) in the under-dose, optimum-dose, and over-dose ranges. This rheological information on the additional shear would be useful to achieve the highest cake solids at the lowest possible polymer dose and operational costs. Wang and Dentel (2011) observed that the extended mixing intensity did not have a distinct effect on the capillary suction time (CST) of conditioned anaerobic digested sludge (ADS) at specific polymer dosages. After sludge flocs were destroyed by the additional shearing, the possible regrowth of the broken flocs could reduce the optimum dosage requirement for their conditioning. However our understanding of the effect of additional shear on the reversibility of the structure and dewatering of sewage sludge remains limited.

Coagulation is a well-established process in water treatment for removing suspended particles by combining small particles into larger aggregates. In comparison with sewage sludge, the floc matrix obtained from coagulation is a type of dilute suspension with many inorganic components. Many studies have shown that floc regrowth after exposure to high shear was limited for all the investigated flocs, including Fe precipitate, Fe-NOM, Al-NOM (Jarvis et al., 2005a), Al-humics, PACl-humics (Wang et al., 2009), nano-Al_{13} polymer and PACl coagulated flocs (Xu et al., 2010), kaolin flocs (Yukselen and Gregory, 2002, 2004a, 2004b; Li et al., 2007; Yu et al., 2011), and natural organic matter (NOM) flocs (Jarvis et al., 2005a; Wang et al., 2009; Xu et al., 2010; Yu et al., 2010, 2012). To repair the rupture of chemical bonds within the hydroxide precipitates and improve their regrowth ability, a small additional dosage of alum (Yu et al., 2010, 2012) was proven effective. On the other hand, Yukselen and Gregory (2004b) observed that clay particles flocculated with a cationic polyelectrolyte presented almost completely reversible floc breakage. Wei et al. (2010) compared the regrowth capacity of flocs formed by different polyferric–polymer dual coagulants and suggested that the charge neutralization and bridging of the cationic polymer PDADMAC is the dominant driving force in the recovery of broken flocs.

Sewage sludge shows many differences in content, components, and structure in coagulation compared to the aforementioned flocs. Biggs and Lant (2000) studied the effect of shear on activated sludge (AS) flocculation and determined the correlation between shear strength and AS size. Yuan and Farnood (2010) investigated the breakage of raw AS flocs under turbulent shear conditions as a function of floc size. They obtained the shear stress distribution functions for the breakage of AS floc samples. Despite the aforementioned advancements in the breakage and regrowth of flocs in water treatment, the corresponding research on sewage sludge, especially for the regrowth of broken aggregates, remains limited. The reversibility of the structure and dewatering of raw and conditioned sewage sludge aggregates owing to additional shear affects the conditioning strategy, which is of fundamental and practical significance in sewage sludge treatment and management. Clearly, these phenomena warrant further investigation.

This study aims to investigate the reversibility of structure and dewaterability of raw, optimally dosed, and overdosed ADS during the continuous strong shear–self-regrowth (CSS–SR) or multipulse shear–self-regrowth (MPS–SR) processes.

The changes in the zeta potential, size (d_{50}), mass fractal dimension (D_F), and CST of ADS aggregates during the aforementioned processes was recorded to assess the self-recovery in the structure and dewaterability of the broken ADS flocs under slow mixing. An improved understanding of this process would be an important contribution to the field of sewage sludge conditioning and dewatering.

1. Materials and methods

1.1. Raw sludge

The raw ADS tested was collected from a wastewater treatment plant in Beijing, China, which handles 1,000,000 m^3 wastewater per day by using a traditional two-stage activated sludge process. The ADS samples were taken from the anaerobic digestion tank and then they were immediately transferred to the laboratory at Beijing Forestry University and stored at 4 °C. Subsequently, experiments were conducted within a week after sampling. Prior to each experiment, the ADS samples were warmed to 25 °C. The total suspended solids (TSS) and volatile suspended solids (VSS) in ADS were determined according to APHA (American Public Health Association) (2005). The CST was measured with a capillary suction timer (Z304M, Triton Electronic Ltd., USA) to represent ADS dewaterability. The characteristics of the ADS samples are presented in Table 1.

1.2. ADS conditioning

Cationic polyacrylamide WD4960 was chosen as conditioner, with a molecular weight of 20–25 MDa and surface charge density of +2.53 meq/g TS. During the experiments, 0.5% stock solution of WD4960 was prepared and renewed every 24 hr.

Conditioning was conducted with a six-paddle stirring apparatus (JTY-6, Tangshan Dachang Chemicals Ltd., China) as follows: an aliquot of 0.5% WD4960 solution was injected into a 1.0 L beaker full of 500 mL raw ADS within 5 sec of agitation at 800 r/min. Then, the mixture was stirred for 1 min at 800 r/min and for 5 min at 62 r/min. The optimum WD4960 dosage was 2.9–3.5 g/kg TSS, when the CST of the conditioned ADS reached the minimum of 7–10 sec. In addition, a WD4960 dosage of 6.0–7.2 g/kg TSS was considered as an over-dosage during ADS conditioning. All the jar tests were conducted in triplicate to ensure consistency.

Sample	CST (sec)	pH	TSS (g/L)	VSS (g/L)	VSS/TSS
1	931.6 ± 212.8	7.7 ± 0.10	37.7 ± 0.3	24.0 ± 0.2	64%
2	877.6 ± 70.2	7.5 ± 0.02	36.6 ± 0.4	23.3 ± 0.1	64%
3	630.0 ± 48.8	7.6 ± 0.01	41.4 ± 0.3	25.2 ± 0.1	61%
4	842.2 ± 79.2	7.3 ± 0.03	40.1 ± 0.2	25.3 ± 0.3	63%
5	456.4 ± 85.6	7.4 ± 0.04	34.6 ± 1.6	21.7 ± 0.8	63%

Table 1 – Characterization of anaerobic digested sludge (ADS).

CST: capillary suction time, TSS: total suspended solid, VSS: volatile suspended solid.

1.3. Breakage and self-regrowth of ADS

In this study, two shear modes, CSS–SR and MPS–SR, were imposed for the breakage and regrowth of ADS aggregates. The corresponding experiments were conducted with an IKA-2000 cantilever agitator (EUROSTAR 20 digital, IKA, Germany) and 1 L jar with 500 mL ADS. In the CSS–SR mode, ADS was first stirred at 400–1200 r/min for 1 min to break the ADS aggregates, and then to 62 r/min for 15 min to recover the broken aggregates. In the MPS–SR mode, ADS was successively stirred six times, and each stirring cycle consisted of 10 sec shearing at 1200 r/min and 1 min shearing at 62 r/min. After the MPS stage, the sheared ADS aggregates were stirred at 62 r/min for another 15 min to allow them to regrow. ADS samples 1–4 in Table 1 were used in the CSS–SR tests, and sample 5 in the MPS–SR tests. During each shear mode, ADS flocs/aggregates were withdrawn before and immediately after breakage, and at the end of every 3 min of self-regrowth. The CST value of each ADS sample was determined immediately. The particle-size distribution was measured by using a laser diffraction instrument (Mastersizer 2000, Malvern, UK, measurement range of 0.02–2000 μm). Subsequently, the aforementioned ADS samples were centrifuged at 3000 r/min for 15 min, and the zeta potential of the colloidal biosolids in the supernatant was examined with a Zetasizer 2000 (Malvern, UK) following the methods proposed by Dursun (2007).

In addition, the average velocity gradient G is commonly used to characterize the turbulent shear rate (Jarvis et al., 2005a) as in the following equation:

$$G = \sqrt{\frac{\varepsilon}{\nu}} \qquad (1)$$

where ε is the energy dissipation rate and ν is the kinematic viscosity of fluid. According to previous publications (Thomas et al., 1999; Yuan and Farnood, 2010), the breakage mechanism of flocs is controlled by the Kolmogorov microscale, λ:

$$\lambda = \left(\frac{\nu^3}{\varepsilon}\right)^{\frac{1}{4}} \qquad (2)$$

For flocs with characteristic length d, it is suggested that under inertial subrange conditions ($d >> \lambda$), flocs are more likely to break by large-scale fragmentation, while surface erosion is proposed to dominate the breakup in the viscous subrange ($d << \lambda$).

G was calculated according to the relation between G and the rotary speed proposed by Hermawan et al. (2004), and the corresponding values of G and λ are presented in Table 2.

1.4. ADS aggregates characterization

The d_{50}, D_F and floc strength (strength factor and recovery factor) of the ADS aggregates were derived from the aforementioned particle size distribution data during the breakage-regrowth process.

The principles for the D_F determination were proposed by Spicer et al. (1998). During the process of small-angle light-scattering tests, the light beam passes through the sample pool, and the particle size in the sample pool is proportional to the scattered light. The scattered light intensity (I) is a function of the scattering vector Q, which is the difference between the incident and scattered light in the medium. Q is given by Eq. (3)

$$Q = \frac{4\pi n \sin(\theta/2)}{\lambda} \qquad (3)$$

where n is the refractive index of the suspending medium, θ is the scattering angle, and λ is the wavelength of the radiation in vacuum. For independent scattering, I is related to Q and D_F in Eq. (4):

$$I \propto Q^{-D_F} \qquad (4)$$

Therefore, D_F can be calculated by using linear regression between I and Q at logarithmic scale.

Based on previous studies (Yukselen and Gregory, 2002; Wei et al., 2010; Francois, 1987; Jarvis et al., 2005b), the breakage factor (BF, %) and regrowth factor (RF, %) are defined as follows:

$$BF = \frac{d_2}{d_1} \times 100\% \qquad (5)$$

$$RF = \frac{d_3 - d_2}{d_1 - d_2} \times 100\% \qquad (6)$$

where d_1 and d_2 represent the floc size before and after breakage and d_3 represents the stable floc size after regrowth.

2. Results

2.1. Zeta potential of ADS

Fig. 1 shows the change in zeta potential of the ADS biosolids under different shear modes. As shown in Fig. 1a, the zeta potentials of raw ADS fluctuated around the initial value of −9.7 mV after CSS, and continued to fluctuate during the subsequent self-regrowth phase. For the conditioned ADS at the optimum WD4960 dosage, the CSS treatment markedly decreased the zeta potential from the initial value of −6.3 mV to around −8.4 mV. The subsequent slow mixing slightly increased the zeta potentials of the sheared ADS at 400 and 700 r/min, whereas it did not change them at 1000 and 1200 r/min. For the ADS conditioned at an overdosage of WD4960, the zeta potential sharply decreased from the initial value of 12.1 mV to −0.3, −5.9, −7.1, and −8.1 mV after the CSS operation at 400, 700, 1000, and 1200 r/min, respectively. The following slow agitation for 15 min at 62 r/min changed the aforementioned zeta potentials to −7.4 mV. In addition, for the ADS after the CSS operation at 400 r/min shearing, the first slow mixing for 3 min at 62 r/min slightly increased the zeta potential, and the subsequent slow mixing for 6 min rapidly reduced the zeta potential to −6.2 mV; thereafter, the zeta potential gradually approached a stable value.

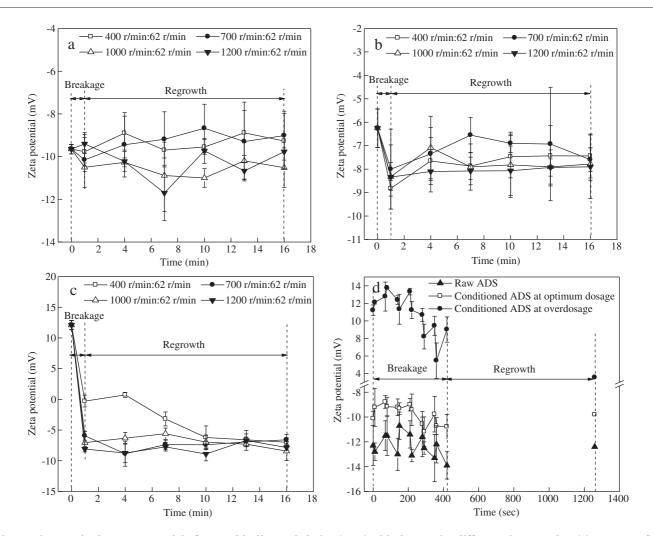| Table 2 – Average velocity gradient (G) and Kolmogorov microscale (λ) values at different rotary speeds.		
Rotation speed (r/min)	G (sec^{-1})	λ (μm)
62	29.4	185.4
400	482.1	45.8
700	1116.0	30.1
1000	1905.6	23.0
1200	2504.9	20.1

Fig. 1 – Changes in the zeta potential of anaerobic digested sludge (ADS) with time under different shear modes. (a) Raw ADS, (b) optimum dosage-conditioned ADS, (c) overdosage-conditioned ADS under the continuous strong shear (CSS)–self-regrowth (SR) mode, and (d) raw and conditioned ADS under the multipulse shear (MPS)–SR mode.

In the MPS–SR mode, the zeta potentials of raw and conditioned ADS at the optimum WD4960 dosage fluctuated during the MPS phase, and then showed slight increase during the subsequent slow mixing phase. For the ADS conditioned at an overdosage of WD4960, its zeta potential decreased from the initial value of 11.2 mV to 9.0 mV after the MPS operation. This suggests that the subsequent 1 min mixing at 62 r/min can slow the decrease in the zeta potential caused by the 10 sec strong shearing at 1200 r/min in the MPS cycle. After the slow mixing phase in the MPS–SR mode, the corresponding zeta potential decreased to 3.6 mV.

2.2. Geometric characteristics of ADS

2.2.1. ADS floc size
The change in ADS floc size (d_{50}) under different shear modes is shown in Fig. 2. As shown in Fig. 2a, the d_{50} of raw ADS was 56.5 μm and slightly decreased to 48.9–51.9 μm after the shear phase. Breakage can be attributed to surface erosion (Francois, 1987). Combined with Fig. 1a, it can be seen that little fresh surface of raw ADS was exposed owing to strong shear. The

subsequent slow mixing slightly increased the d_{50} values of broken raw ADS samples after 400, 700, and 1000 r/min shearing. For the conditioned ADS at the optimum WD4960 dosage, d_{50} sharply decreased from the initial value of 630 μm to 391, 300, 250, and 198 μm after 400, 700, 1000, and 1200 r/min shearing, respectively. This suggests that the breakage mechanism passed from small-scale surface erosion to large-scale fragmentation as the shearing rate increased. The subsequent slow mixing could lead to the flocculation of the broken ADS aggregates after 400 or 700 r/min shearing, and the self-regrown ADS aggregates approached 572 and 420 μm, respectively, which is smaller than their initial size. For the broken ADS aggregates after 1000 and 1200 r/min shearing, self-regrowth did not occur during the subsequent 15 min slow mixing at 62 r/min. As the ADS conditioned at an overdosage of WD4960 was subjected to CSS treatment after 400 r/min, the size of some initial and broken aggregates was close to the measurement limit of the Mastersizer 2000, so that the corresponding d_{50} values do not show in Fig. 3c. After 700, 1000, and 1200 rpm shearing under CSS mode, the d_{50} values of broken aggregates were 644, 409, and 317 μm,
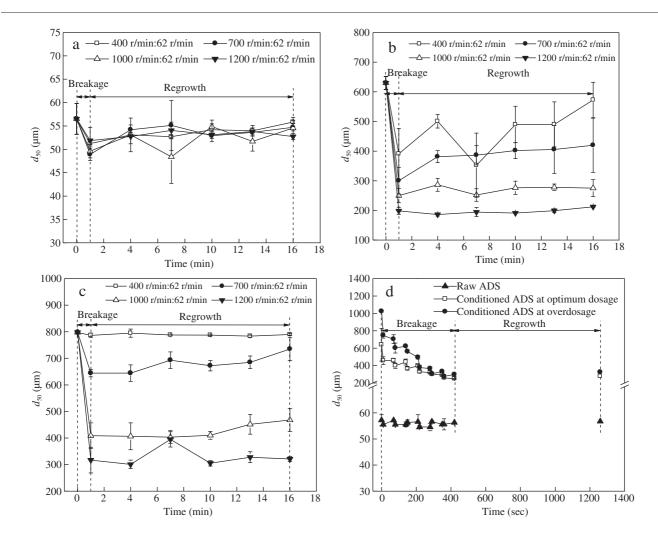
Fig. 2 – Change in the floc size (d_{50}) of ADS with time under different shear modes.(a) Raw ADS, (b) optimum dosage-conditioned ADS, (c) overdosage-conditioned ADS under CSS–SR mode, and (d) raw and conditioned ADS under MPS–SR mode.

respectively. This observation suggested that large-scale fragmentation occurred at 1000 and 1200 r/min shearing.

In the MPS–SR mode, the raw ADS did not show noticeable change in d_{50} during breakage and self-regrowth. For the conditioned ADS at the optimum WD4960 dosage, d_{50} sharply decreased from the initial value of 639 to 248 μm after the MPS operation. Then, the subsequent slow mixing did not lead to significant regrowth of the broken ADS aggregates, and the corresponding d_{50} value was maintained at around 278 μm. The d_{50} value of ADS conditioned at an overdosage of WD4960 also decreased to 297 μm; after the regrowth phase, it was about 325 μm. During the MPS process, the partial recovery caused by 1 min slow mixing at 62 r/min was seen at the 2nd and 3rd cycles for the conditioned ADS at the optimum WD4960 dosage, and the 5th and 6th cycles for the ADS conditioned at an overdosage of WD4960.

2.2.2. Fractal dimension of ADS flocs/aggregates

Fig. 3 shows the change in the D_F of the ADS flocs/aggregates with time under different shear modes. As shown in Fig. 3a, the D_F of raw ADS was 2.12. The CSS treatment did not change

the structure of raw ADS, and the corresponding D_F values fluctuated around 2.07–2.13. For the conditioned ADS at the optimum WD4960 dosage, the initial D_F value was 2.15 and slightly changed after the CSS treatment at different speeds. Then, the subsequent slow mixing only increased the D_F values of broken ADS aggregates after 700, 1000, and 1200 r/min shearing to around 2.20. For the ADS conditioned at an overdosage of WD4960, the D_F value could not be determined due to the size of some aggregates exceeding the measurement capability of the Mastersizer 2000. As shown in Fig. 3c, the D_F values were stable in the following slow mixing phase. The larger ADS flocs/aggregates were, the lower the D_F values were, and the looser the structure was.

In the MPS–SR mode, the D_F value of raw ADS slightly increased during the MPS phase, and then was stable at 2.33 during the subsequent 15 min slow mixing phase. For the conditioned ADS at the optimum WD4960 dosage, the first 10 sec of strong shear decreased the D_F value from 2.35 to 2.12, and then the D_F value increased and reached 2.22 at the end of the MPS phase. Hereafter, the slow mixing led to a slight increase in the D_F value. For the ADS conditioned at an
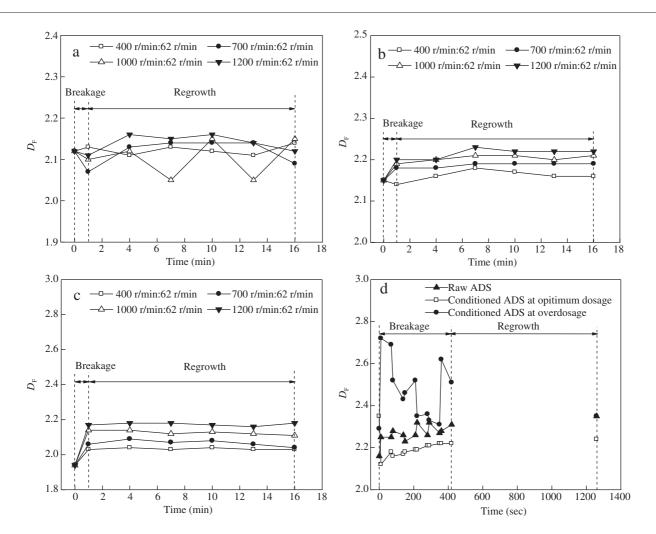
Fig. 3 – Change in the fractal dimension of ADS with time under different shear modes.(a) Raw ADS, (b) optimum dosage-conditioned ADS, (c) overdosage-conditioned ADS under CSS–SR mode, and (d) raw and conditioned ADS under MPS–SR mode.

overdosage of WD4960, the D_F value was 2.51 after MPS shearing. During the regrowth phase, the D_F value continuously decreased to 2.35.

2.2.3. Flocs/aggregates strength

Using Eqs. (5) and (6), the BF and RF of ADS aggregates during CSS–SR and MPS–SR are calculated in Table 3. The d_3/d_1 values also show recovery for broken ADS aggregates. For the raw ADS aggregates, the BF was maintained around 90% after CSS or MPS, indicating that the raw aggregates were insensitive to shearing. In the CSS operation, the BF value of the conditioned ADS at the optimum WD4960 dosage was lower than that of the

overdose-conditioned ADS, and the BF values of both ADS aggregates decreased with increasing shear strength. This suggests that the conditioned ADS at the optimum WD4960 dosage was more easily disrupted by CSS than the overdosage-conditioned ADS. Moreover, the RF value of the broken aggregates of conditioned ADS at the optimum WD4960 dosage was 76% after 400 r/min CSS. The corresponding d_3/d_1 value reached 91%, thus suggesting high recovery. Meanwhile, the RF values of the broken aggregates were 7% and 3% after strong shearing, thereby indicating insignificant recovery. For the broken fragments of overdosed ADS aggregates, the RF values in Table 3 showed that the recovery was not very strong. The aforementioned result

Table 3 – Breakage factor (BF) and recovery factor (RF) of ADS aggregates.							
			Raw ADS		Optimally dosed ADS		Overdosed ADS
Shear mode	G (sec^{-1})	BF (%)	RF/(100 × d_3/d_1) (%)	BF (%)	RF/(100 × d_3/d_1) (%)	BF (%)	RF/(100 × d_3/d_1) (%)
CSS–SR	482.1	91	87/99	62	76/91	–	–
	1116.0	87	76/97	48	36/67	–	–
	1905.6	88	72/97	40	7/44	51	15/59
MPS–SR	2504.9	92	18/93	32	3/34	40	1/40
	2504.9	98	51/99	39	8/43	–	–

shows that CSS does not favor the self-regrowth of broken fragments from overdosed ADS. CSS performed worse than MPS with respect to the broken fragments from optimally dosed ADS.

2.3. Change in the dewaterability of ADS

Fig. 4 shows the dewaterability variation of raw and conditioned ADS with time under different shear modes. As shown in Fig. 4a, the initial CST value of raw ADS was 686.2 sec, and both CSS and slow mixing led to the fluctuation of the CST values of raw ADS, with a corresponding average value of about 728.9 s with large deviation. In Fig. 4b, the CST values of conditioned ADS at the optimum WD4960 dosage increased from 11.5 sec to 19.2, 23.8, 40, and 44.4 sec after 400, 700, 1000, and 1200 r/min CSS treatment, respectively. The subsequent slow mixing resulted in decreasing CST values for the aforementioned ADS samples. However, the final CST values after slow mixing did not recover to the initial CST value of 11.5 sec. For the ADS conditioned at an overdosage of WD4960, the CST values decreased from 44 sec to 7.3, 7.8, 9.2, and 11.7 sec after 400, 700, 1000, and 1200 r/min CSS, respectively. Then, they remained stable during the following slow mixing phase.

In the MPS–SR mode, the CST value of raw ADS fluctuated during the MPS phase, and once reached 520.8 sec, which is higher than the initial value of 456.4 sec. The following slow mixing finally reduced the CST value to 379.8 sec. For the conditioned ADS at the optimum WD4960 dosage, the CST value increased several to tens of seconds at each 10 sec of strong shearing at 1200 r/min, and decreased a few seconds at each slow mixing for 1 min at 62 r/min afterwards. At the end of the MPS operation, the CST value increased from 10.6 to 28.6 sec. This value was stable during the following slow mixing for 15 min. As the ADS was conditioned at an overdosage of WD4960, the CST value decreased from 54.6 to 8.8 sec during the MPS operation, and then remained at 8 sec during the subsequent slow mixing. Moreover, the increase of CST at each slow mixing phase for 1 min was less than the decrease at the corresponding 10 sec strong shearing phase.

3. Discussion

As indicated in Table 2, λ decreased from 45.8 to 20.1 μm as the G value increased from 482.1 to 2504.9 sec^{-1}. This value
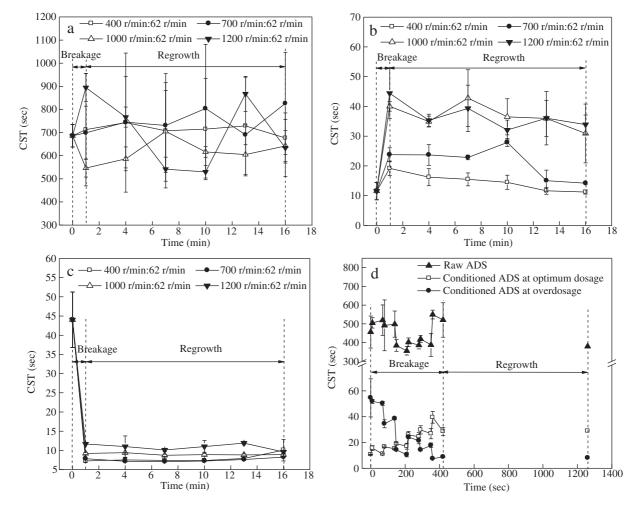

Fig. 4 – Changes in CST of ADS with time under different shear modes.(a) Raw ADS, (b) optimum dosage-conditioned ADS, (c) overdosage-conditioned ADS under CSS–SR mode, and (d) raw and conditioned ADS under MPS–SR mode.

was within the size distribution range of raw ADS (d_{10} to d_{90} of 16.5 μm to 159.9 μm). This finding implied that the slight breakage of raw ADS aggregates can be ascribed to the surface erosion mechanism.

As shown in Fig. 1, both CSS and MPS resulted in decreasing the zeta potential of conditioned ADS, which implied that the fresh negatively charged surface within the conditioned ADS was exposed after shearing. Dentel (2001) indicated that raw sludge flocs are fragile and easily disrupted when conditioned sludge aggregates are sheared. Therefore, the aforementioned fresh negatively charged surface could be attributed to the disruption of raw ADS during CSS or MPS. However, the zeta potential of broken ADS aggregates could not approach the value of raw ADS owing to the charge neutralization effect of the WD4960-conditioned surface. In addition, this effect was more obvious in overdosed ADS aggregates after breakage than for the optimally dosed ones. In addition, during the MPS phase, the fresh negatively charged surface on the overdosed ADS after 10 sec of strong shear could be partially neutralized by the WD4960-conditioned surface during the subsequent mixing for 1 min at 62 r/min. Also, in most cases, 15 min mixing at 62 r/min led to stable zeta potential values for the conditioned ADS during the self-regrowth phase.

In the current study, the size distributions of the optimally dosed and overdosed ADS aggregates ranged from 163.2 μm to >1.2 mm and 564.6 μm to >1.2 mm in terms of d_{10} to d_{90}, respectively. According to the proposals of Thomas et al. (1999) and Yuan and Farnood (2010), the breakage of conditioned ADS aggregates can be attributed to both surface erosion and large-scale fragmentation.

Based on the curves in Fig. 2, it can be seen that the d_{50} values of the conditioned ADS after CSS or MPS decreased to no less than 200 μm, which was more than three times larger than that of the raw ADS. This finding implied that energy dissipation of the Kolmogorov microscale eddies during either CSS or MPS was insufficient to disrupt the fragments of conditioned ADS further. Moreover, the subsequent 15 min mixing at 62 r/min did not recover the initial value of conditioned ADS. As shown in Fig. 3, in most cases, both the broken and the regrown ADS aggregates during CSS–SR or MPS–SR were more compact than the initial conditioned ones.

The findings in Table 3 indicate that the conditioned ADS displayed irreversible floc breakage, except for $G = 482.1$ sec^{-1}. This result was inconsistent with the observation of Yukselen and Gregory (2004b). For clay particles flocculated with a cationic polyelectrolyte (Yukselen and Gregory, 2004b), primary particles are bound by electrostatic-type, van der Waals-type, and DLVO-type forces (Yuan and Farnood, 2010). However, EPS entanglement is crucial in the cohesion forces within AS and ADS flocs (Mikkelsen and Nielsen, 2001) or anaerobic granules (Wu et al., 2009, 2012). Moreover, Wu et al. (2009) observed that a typical shear rate of 8.3 sec^{-1} could stimulate extracellular protein secretion to enhance nucleation, whereas Wu et al. (2012) reported that high shear rate and short interval between two contiguous shear conditions inhibited the extracellular polymer production and bioactivity in upflow anaerobic reactors fed with glucose solution, then disrupted the anaerobic granules. In this study, the ADS was used to conduct breakage and self-regrowth experiments without a feeding nutrient matrix. The EPS exposed by the

breakage of ADS took on a negative charge and did not promptly flocculate the fragments under the bridging mechanism during the 15-min slow mixing period. When ADS was broken, fresh surface was exposed with negative charge. The optimally dosed or overdosed WD4960 played charge neutralization and bridging roles in flocculation of ADS flocs with high solid content. No residual WD4960 remained to neutralize the negative charge of the fresh surface and perform bridge flocculation further; this charge can be neutralized slightly by the conditioned surface of ADS. Therefore, reflocculation and corresponding self-growth did not occur among the broken fragments.

For the conditioned ADS at the optimum dosage, CSS or MPS treatment deteriorated dewaterability, and the subsequent 15 min mixing at 62 r/min did not recover the initial CST before breakage. However, the dewaterability of the overdosage-conditioned ADS improved after CSS or MPS, and then remained stable during the following slow mixing phase.

4. Conclusions

Raw ADS was insensitive to CSS–SR or MPS–SR treatment; d_{50} decreased less than 10 μm after breakage. For the conditioned ADS, both MPS and CSS generally yielded small and relatively compact fragments with exposed negatively charged fresh surfaces, and the MPS-treated ADS had larger and more compact fragments with lower CST than the CSS-treated ADS. During the subsequent slow mixing, the broken ADS aggregates were irreversibly changed in terms of structure and dewaterability. The breakage of overdosed ADS decreased CST, which suggested that overdosage conditioning may counteract the shear experienced by the conditioned ADS. In the ADS dewatering, the optimum cationic polyacrylamide dosage for conditioning determined by Jar test was an under-dose in practice due to the additional shearing. It is better to employ an over-dose based on Jar test values for practical conditioning to weaken the adverse effects of additional shearing.

REFERENCES

Abu-Orf, M.M., Dentel, S.K., 1997. Effect of mixing on the rheological characteristics of conditioned sludge: full-scale studies. Water Sci. Technol. 36 (11), 51–60.

APHA (American Public Health Association), 2005. Standard Methods for the Examination of Water and Wastewater. 21st ed. American Public Health Association, American Water Works Association and Water Environment Federation, Washington, DC, USA.

Biggs, C.A., Lant, P.A., 2000. Activated sludge flocculation: on-line determination of floc size and the effect of shear. Water Res. 34 (9), 2542–2550.

Dentel, S.K., 2001. Conditioning. In: Spinosa, S., Vesilind, P.A. (Eds.), Sludge into Biosolids Processing, Disposal and Utilization, 1st ed. IWA Publishing, London, pp. 279–314.

Dursun, D., 2007. Gel-like Behavior of Biosolids in Conditioning and Dewatering Processes. University of Delaware.

Francois, R.J., 1987. Strength of aluminium hydroxide flocs. Water Res. 21 (9), 1023–1030.

Hermawan, M., Bushell, G.C., Craig, V.S.J., Teoh, W.Y., Amal, R., 2004. Floc strength characterization technique: an insight into silica aggregation. Langmuir 20 (15), 6450–6457.

Jarvis, P., Jefferson, B., Parsons, S.A., 2005a. Breakage, re-growth, and fractal nature of natural organic matter flocs. Environ. Sci. Technol. 39 (7), 2307–2314.

Jarvis, P., Jefferson, B., Gregory, J., Parsons, S.A., 2005b. A review of floc strength and breakage. Water Res. 39 (14), 3121–3137.

Li, T., Zhu, Z., Wang, D.S., Yao, C.H., Tang, H.X., 2007. The strength and fractal dimension characteristics of alum–kaolin flocs. Int. J. Miner. Process. 82 (1), 23–29.

Mikkelsen, L.H., Nielsen, P.H., 2001. Quantification of the bond energy of bacteria attached to activated sludge floc surfaces. Water Sci. Technol. 43 (6), 67–75.

Novak, J.T., 1990. The effect of mixing on the performance of sludge conditioning chemicals. Water Supply 8, 53–60.

Novak, J.T., Bandak, N., 1989. Chemical conditioning and the resistance of sludges to shear. J. Water Pollut. Control Fed. 61 (13), 327–332.

Novak, J.T., Predenville, J.F., Sherrard, J.H., 1988. Mixing intensity and polymer performance in sludge dewatering. J. Environ. Eng. 114 (1), 190–198.

Örmeci, B., Ahmad, A., 2009. Measurement of additional shear during sludge conditioning and dewatering. Water Res. 43 (13), 3249–3260.

Spicer, P.T., Pratsinis, S.E., Raper, J., Amal, R., Bushell, G., Meesters, G., 1998. Effect of shear schedule on particle size, density, and structure during flocculation in stirred tanks. Powder Technol. 97 (1), 26–34.

Thomas, D.N., Judd, S.J., Fawcett, N., 1999. Flocculation modeling: a review. Water Res. 33 (7), 1579–1592.

Wang, Y.L., Dentel, S.K., 2011. The effect of polymer doses and extended mixing intensity on the geometric and rheological characteristics of conditioned anaerobic digested sludge (ADS). Chem. Eng. J. 166 (3), 850–858.

Wang, Y., Gao, B., Xu, X., Xu, W., Xu, G., 2009. Characterization of floc size, strength and structure in various aluminum coagulants treatment. J. Colloid Interface Sci. 332 (2), 354–359.

Wei, J.C., Gao, B.Y., Yue, Q.Y., Wang, Y., 2010. Strength and regrowth properties of polyferric–polymer dual-coagulant flocs in surface water treatment. J. Hazard. Mater. 175 (1-3), 949–954.

Werle, C.P., Novak, J.T., Knocke, W.R., Sherrard, J.H., 1984. Mixing intensity and polymer sludge conditioning. J. Environ. Eng. 110 (5), 919–934.

Wu, J., Zhou, H.M., Li, H.Z., Zhang, P.C., Jiang, J., 2009. Impacts of hydrodynamic shear force on nucleation of flocculent sludge in anaerobic reactor. Water Res. 43 (12), 3029–3036.

Wu, J., Bi, L., Zhang, J.B., Poncin, S., Cao, Z.P., Li, H.Z., 2012. Effects of increase modes of shear force on granule disruptionin upflow anaerobic reactors. Water Res. 46 (10), 3189–3196.

Xu, W., Gao, B., Yue, Q., Wang, Y., 2010. Effect of shear force and solution pH on flocs breakage and re-growth formed by nano-Al13 polymer. Water Res. 44 (6), 1893–1899.

Yu, W.Z., Gregory, J., Campos, L., 2010. Breakage, regrowth of Al-humic flocs—effect of additional coagulant dosage. Environ. Sci. Technol. 44 (16), 6371–6376.

Yu, W.Z., Gregory, J., Campos, L., Li, G.B., 2011. The role of mixing conditions on floc growth, breakage and re-growth. Chem. Eng. J. 171 (2), 425–430.

Yu, W.Z., Hu, C.Z., Liu, H.J., Qu, J.H., 2012. Effect of dosage strategy on Al-humic flocs growth and re-growth. Colloids Surf. A Physicochem. Eng. Asp. 404, 106–111.

Yuan, Y., Farnood, R.R., 2010. Strength and breakage of activated sludge flocs. Powder Technol. 199 (2), 111–119.

Yukselen, M.A., Gregory, J., 2002. Breakage and reformation of alum flocs. Environ. Eng. Sci. 19 (4), 229–236.

Yukselen, M.A., Gregory, J., 2004a. The effect of rapid mixing on the break-up and re-formation of flocs. J. Chem. Technol. Biotechnol. 79 (7), 782–788.

Yukselen, M.A., Gregory, J., 2004b. The reversibility of flocs breakage. Int. J. Miner. Process. 73 (2-4), 251–259.